Modelling of Vortex based Hydrodynamic Cavitation Reactors

Varaha Prasad Sarvothaman, Alister Thomas Simpson and Vivek Vinayak Ranade*

School of Chemistry and Chemical Engineering

Queen's University Belfast

Belfast BT9 5AG, Northern Ireland, United Kingdom.

*Corresponding author: V.Ranade@qub.ac.uk

Submitted for ISCRE25 Special Issue of Chemical Engineering Journal

Abstract

Vortex based hydrodynamic cavitation reactors offer various advantages like early inception, less erosion and higher cavitational yield. No systematic modelling efforts have been reported to interpret the cavitation performance of these vortex based devices for cavitation. It is essential to develop a modelling framework for describing performance of cavitation reactors. We have addressed this need in the present work. A comprehensive modelling framework comprising three layers: per – pass performance models (overall process), computational fluid dynamics models (flow on reactor scale) and cavity dynamics models (cavity scale) is developed. The approach and computational models were evaluated using the experimental data on treatment of acetone-contaminated water. The presented models were successful in describing the experimental data using initial cavity size as an adjustable parameter. Efforts were made to quantify optimum operating conditions and scale-up. The developed approach, models and results will provide useful design guidelines for pollutant degradation using vortex based cavitation reactors. It will also provide a sound and useful basis for comprehensive multi-scale modelling of hydrodynamic cavitation reactors.

Keywords: Hydrodynamic Cavitation; Vortex based devices; Effluent Treatment; Modelling.

1. Introduction

Cavitation is the formation, growth and implosion of bubbles in a liquid medium undergoing variation in pressure (Capocelli et al., 2014). The implosion of these bubbles leads to extreme temperatures and pressures in a tiny volume. These extreme temperatures (> 2000 K) and pressures (> 100 MPa) results in highly reactive radical species (from water and dissolved air). Among the radicals formed during the collapse, the hydroxyl radicals (OH) have a very high oxidising ability. This can be harnessed for a variety of applications. Of the variety of ways with which cavitation can be realised in practice, hydrodynamic cavitation is most relevant for industrial applications particularly at larger scale (Pradhan and Gogate 2010; Chakinala et al., 2009; Jyoti and Pandit, 2001). In this work, we restrict the scope to discuss hydrodynamic cavitation.

Hydrodynamic cavitation is realised by designing a cavitation device or reactor in such a way that it generates low pressure regions within the reactor where pressure falls below the vapour pressure of liquid. This leads to the formation of vaporous cavities. These cavities are then transported in a region of higher pressure where cavities collapse. As mentioned above, collapsing cavities generate highly reactive hydroxyl radicals which can then be harnessed for a variety of applications. One of the most widely investigated application of hydrodynamic cavitation is wastewater treatment (see Ranade and Bhandari, 2014 and references cited therein; Gagol et al. 2018). Several other applications of cavitation have also been reported (Carpenter et al. 2017; Suryawanshi et al., 2017, 2018; Ranade et al., 2017, 2016; Pathania et al. 2018 and references cited therein). Hydrodynamic cavitation offers several advantages such as no additional chemicals (clean tech), compact and in-line reactors and low costs. This makes it a very promising technology platform.

Despite significant research on hydrodynamic cavitation (more than 4000 publications on hydrodynamic cavitation per year are listed by Google Scholar), the excellent promise of this technology has not yet been fully realised in practice. There are mainly two reasons for this scenario:

1. Designs of cavitation reactor: Conventionally hydrodynamic cavitation reactors are designed either using small constrictions (like orifices or venturi) or rotors to realise the desired low pressure regions for generating cavitation. Orifice or venturi based designs are susceptible to clogging and erosion since cavitation occurs close to solid walls (see for example, Simpson and Ranade, 2018a). Reactors based on rotors are expensive and impose higher operating and maintenance costs (Gogate and Pandit, 2001). New designs that overcome some of these limitations are needed.
2. Lack of systematic design, optimisation and scale-up methodologies: Though there are several published studies using orifice and venturi based cavitation reactors, most of the studies use in-house designs of orifice and venturi (number of holes, thickness of orifice plates, and sharpness of orifice, depth of throat of venturi, diffuser angle of venturi and so on). It is therefore difficult to relate results of one study with the other since these devices lack standardisation. It should be noted that small hardware features like thickness of orifice plate and radius of curvature of orifice (see Simpson and Ranade, 2018a) can significantly influence cavitation characteristics. Many times, not all of the relevant dimensions and operating conditions (like cavitation inception conditions, volume of holding tank etc.) are reported making interpretation of results difficult. Results from two different devices are also therefore difficult to relate. Despite so many studies, performance of geometrically similar cavitation devices on different scales is scarce and no systematic guidelines or methodologies are available for design, optimisation and scale-up.

In this work, we have attempted to address these issues and present a systematic design and optimisation process for a recently developed vortex based hydrodynamic cavitation reactor. Key features of vortex based devices for cavitation (VoDCa) are summarised here for the sake of

completeness. Published attempts of developing design and optimisation models of cavitation reactors are critically reviewed. The scope of the present work and structure of this presentation are then briefly discussed.

Ranade et al. (2016, 2017) have disclosed vortex based devices for cavitation (VoDCa) which can shield the cavities from the reactor walls and can overcome the limitations of conventional hydrodynamic cavitation (HC) devices. Recent studies report several advantages of VoDCa over cavitation reactors based on orifice or venturi (see for example, Suryawanshi et al. 2017; 2018). VoDCa are now commercially available and have been deployed at scales up to 50 m^3/hr (www.vivira.in; Utikar, 2018). In this work, we investigated design, optimisation and scale – up of VoDCa for the application of treatment of acetone contaminated water. None of the cited studies on VoDCa discuss design and scale – up methodology. Systematic design methodologies are not available even for conventional devices like orifice and venturi despite several attempts of developing these. Published attempts of modelling and design of cavitation reactors is briefly reviewed in the following.

Most of the published studies carry out batch operation (with total recycle) of cavitation reactors. The experimental data obtained from such batch experiments is often interpreted using pseudo-first order kinetics, and rate constants are reported with units of s^{-1} (see for example, Barik and Gogate 2016; Rajoriya et al., 2018 and references cited therein). Several studies have shown that the apparent rate constant of degradation exhibits a maxima with respect to pressure drop across cavitation device (Rajoriya et al., 2017; Thanekar et al., 2018; Capocelli et al., 2014). In order to understand such behaviour of a cavitation reactor, the apparent rate constant (which in reality is function of cavitation device configuration, operating conditions, number of passes through cavitation device and so on) is correlated with results obtained with cavity dynamics models. Extensive work on cavity dynamics models has been done by Pandit – Gogate – Moholkar and their co-workers (see for example, Gireesan and Pandit, 2017; Chakma and Moholkar, 2013; Sharma et al., 2008; Krishnan et al, 2006; Kanthale et

al., 2005 and references cited therein. Krishnan et al. (2006) developed the framework to predict OH generation from collapse conditions. It should be noted that cavity dynamic models involve several sub-models. There are several uncertainties associated with the estimation of transport properties, interface boundary conditions, definition of collapse and so on. The results of the cavity dynamics model are quite sensitive to initial size of the cavity. There have been attempts to include distribution of initial cavity sizes instead of considering a single cavity. For example, Capocelli et al. (2014) used a size distribution of initial cavity size, R_0 in the range of 20 – 250 μm based on the work of Liu and Brennen (1995). Attempts have been made to qualitatively relate the results of cavity dynamics models with the performance of cavitation reactor. Sharma et al. (2008) have developed an empirical correlation for temperature, pressure and radical generation at collapse as a function of initial radius of cavity, inlet pressure to the HC device and diameter of an orifice hole. Unfortunately the applicability of such correlations is quite restricted and different and HC devices are seldom directly comparable (Šarc et al., 2017).

In order to relate the models with the device design and operating parameters, it is essential to connect cavity dynamics models with the fluid dynamics realised in the cavitation reactor. Several attempts have been made towards simulating fluid dynamics of cavitation devices. The flow modelling studies can be broadly divided into two groups: the first group focusses on detailed flow characteristics using sophisticated computational fluid dynamics (CFD) models. For example, Chahine and co-workers (Ma et al. 2017, Hsiao et al. 2017) have presented a multi-scale framework which merges the Lagrangian approach for tracking nuclei and micro-bubbles with the macro-scale Eulerian approach for resolving larger cavities, using a bridging scheme between the disparate scales. These approaches have been shown to be able to successfully reproduce cavity formation. These studies however are far too disconnected with the performance of cavitation reactors. On the other hand, the second group focusses on simulating performance of cavitation reactors using rather simplified CFD models. For example, Capocelli et al. (2014) used a simplified one-dimensional CFD model for flow in cavitating

venturi for qualitatively capturing the trend observed in performance of cavitation reactor. Pawar et al. (2017) have used single phase flow simulations at a single operating condition for four hydrodynamic cavitation devices. It is essential to strike an appropriate balance between these two groups in order to make progress in relating the design and operation of cavitation reactors to degradation performance. Such an attempt is made here. In this work, we have developed a multi-layer modelling approach to relate cavitation reactor performance with its design and operation. We have used a per-pass degradation model presented in our earlier work (Sarvothaman et al. 2018) as a starting point. The experimental data was interpreted with this model to obtained 'per-pass degradation' performance of cavitation reactors under different operating conditions. The experimentally obtained per-pass degradation factor was then estimated using the detailed CFD models of VoDCA (Simpson and Ranade, 2018b) and cavity dynamics models (Pawar et al., 2017; Chakma and Moholkar, 2013; Krishnan et al., 2006). New ways of estimating the number of cavitation events and relating CFD models with the cavity dynamics models are proposed. The approach was used to describe the experimental data with the help of minimum adjustable parameters. The approach and model was able to capture the influence of scale on degradation performance reasonably well. The model was then used to understand possibilities for improving reactor performance. The effect of increasing downstream pressure was found to increase degradation rates. Experiments were performed to verify this observation. The approach and models were then used to simulate the influence of scale of cavitation reactor. The simulated results were compared and discussed with reference to the limited scale – up data available so far. The developed approach can be used to design, optimise and scale-up hydrodynamic cavitation reactors. The key results are discussed after presenting details of experimental work and computational models.

2. Experimental

The experimental setup used in this work is a modification of the experimental setup described in our previous work (Sarvothaman et al., 2018). While the earlier work studied the effect of pressure drop

in the cavitating device, in this work we have also investigated the effect of downstream pressure on degradation performance and the new data is reported. The experimental set-up used in the earlier work was modified to facilitate experiments with different downstream pressures. For this purpose, two valves were installed in the downstream section of the cavitating device (see Figure 1). The use of multiple valves avoids excessive pressure drop across any single valve and avoids the possibility of valve cavitation. The overall liquid volume of the modified setup was 9 L (slightly lower than the volume of 9.3 L used in the previous work).

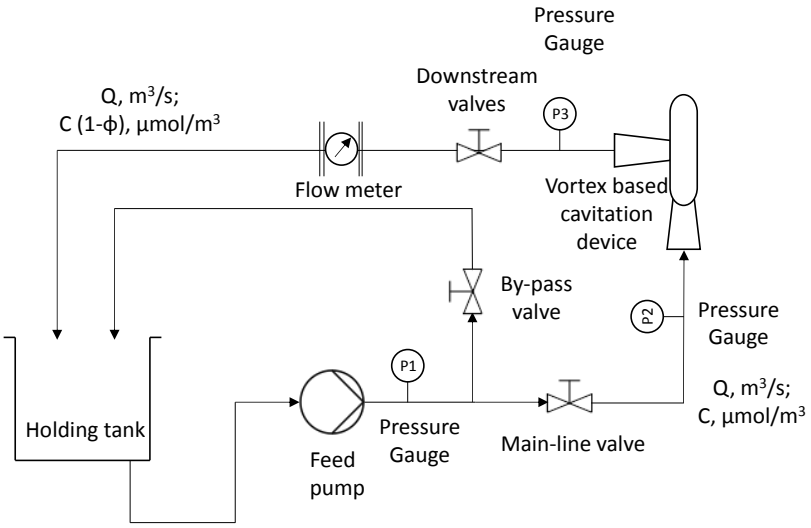

Figure 1: Schematic of experimental set-up

Two similar experimental set-ups were constructed with two geometrically similar vortex based cavitation devices. The cavitation devices were procured from Vivira Process Technologies (www.vivira.in). The key characteristics of the two set-ups are listed in Table 1.

Table 1: Details of two experimental set-ups

Cavitation device	Throat diameter, mm	Nominal capacity, m^3/hr	Working liquid volume, m^3
Small (S)	6	0.3	0.009
Large (L)	12	1.2	0.015

The pressure drop characteristics of these two cavitation devices and the details of experimental procedure are discussed by Sarvothaman et al. (2018). Following the practices established in that work, care was taken to ensure that there is no cavitation in the system other than that in the cavitation device itself. This was ensured by tracking the cavitation noise via stethoscopes. New experimental data was collected for varying downstream pressure of the cavitation reactor for the constant inlet pressure. The analytical methods used to quantify treatment of acetone contaminated water are discussed in the earlier work. The experimental data was processed using the per – pass degradation factor as discussed by Sarvothaman et al. (2018). The data are presented and discussed in Section 4.

3. Modelling of hydrodynamic cavitation reactors

In this work we apply the recently developed per – pass degradation framework (Sarvothaman et al. 2018) for modelling the system shown in Figure 1. Complete mineralisation of pollutant proceeds via a multi-step unstable organic radical formation. There are several attempts to understand radical formation and their subsequent reactions with pollutants (see for example reaction schemes proposed by Saharan et al., 2014). However, these reactions are represented by following commonly used simplification:

$Cavity\ collapse \rightarrow OH^{\cdot} and\ other\ radicals\ (R^{\cdot})$ .....R 1

$R^{\cdot} + pollutant \rightarrow CO_2 + H_2O$ .....R 2

The overall behaviour of a typical cavitation based water treatment set-up shown in Figure 1 can be modelled as:

$$V\frac{dC}{dt} = -Q\emptyset C \quad (1)$$

Where C is a concentration of pollutant, V is a holding tank volume, Q is a flow rate through cavitation device and ϕ is a per-pass degradation factor. The number of passes, n can be related to time as:

$$n = \frac{Q}{V}t \quad (2)$$

If the value of ϕ is assumed to be constant over a range of concentration and time, it can be obtained by running the cavitation set-up in a batch model and using experimental measurement of concentration of pollutant as:

$$C = C_{in}e^{-\emptyset n} \quad (3)$$

Per-pass degradation coefficient, ϕ, can be related to generation of hydroxyl radicals in the cavitation device (G, kmol/s) and their subsequent reactions with the pollutant. Considering that radicals have very small life time compared to the residence time in the cavitation device (and downstream piping up to the holding tank), it may be safely assumed that all radicals are consumed within the reactor. Radicals are highly reactive and therefore in addition to reaction R2, radicals may react with any other scavangers present in the liquid (including water itself). Therefore only a fraction of generated radicals (say, δ) will be used for degrading the pollutant. This fraction may be written as:

$$\delta = \frac{k_2 C}{(k_2 C + k_S C_S)} \quad (4)$$

The per-pass degradation factor can then be related to the generation rate as:

$$Q\ C\ \emptyset = G\ \delta \quad (5)$$

The per-pass degradation coefficient can then be written as:

$$\emptyset = \frac{\left(\frac{G}{Q\ C_S}\right)}{\left(\frac{k_S}{k_2} + \frac{C}{C_S}\right)} \quad (6)$$

The per-pass degradation factor will depend on the generation rate of hydroxyl radicals (G), flow rate through cavitation device (Q), chemical nature of pollutant (reactivity with hydroxyl radicals, k_2), concentration of the pollutant (C), concentration of scavangers (C_S) and the relative rate reactivity of pollutant and scavangers (k_2/k_S) with hydroxyl radicals. It can be seen that for low concentrations of pollutant ($C << C_S$), the value of per-pass degradation factor will be independent of pollutant concentration. It will essentially depend on the effective generation rate of hydroxyl radicals, G and the ratio of k_S to k_2. As the reactivity of pollutant decreases with respect to reactivity of the other existing scavangers, the per-pass degradation factor decreases. Besides applying the per-pass model to describe the experimental data as done by Sarvothaman et al. (2018), here we attempt to further develop the model for estimation of per-pass degradation factor, ϕ.

The radical generation rate, G depends on flow characteristics of the cavitation device which controls number density of cavitation events and intensity of cavity collapse (which controls the generation of hydroxyl radicals per collapsing cavity). The generation rate of hydroxyl radicals may be related to the number of cavities collapsing per second in the cavitation device (n, s^{-1}) and hydroxyl radicals generated per collapse, m_{OH} (kmol) as:

$$G = n\, m_{OH} \qquad \text{kmol/s} \qquad (7)$$

It should be noted that hydroxyl radicals generated per collapse depend on a variety of factors such as initial radius of cavity and bulk pressure fluctuations experienced by cavity (as it is moving within the cavitation device). All the cavities generated will not be of the same initial radius and all the generated cavities (even with those with same initial radius) will not experience same bulk pressure fluctuations because of inherently turbulent flow. It may therefore necessary to introduce a proportionality factor in the above equation. The number of cavities generated per second may be indirectly related to the flow rate through the device, gas volume fraction and representative volume of a cavity as:

$$n \propto \frac{Q\,\epsilon_{GR}}{V_{in}} \qquad s^{-1} \qquad (8)$$

V_{in} is volume of cavity at the inception. The term ϵ_{GR} denotes the effective volume fraction of cavities. It is important to carefully select a region to estimate appropriate value of ϵ_{GR}. This is discussed in Section 4.2.

Substituting Equation (8) into Equation (7) we get,

$$\emptyset \propto \frac{\epsilon_{GR}\left(\frac{C_{OH}}{C_S}\right)}{\left(\frac{k_S}{k_2}+\frac{C}{C_S}\right)} \qquad (9)$$

Where C_{OH} is concentration of the hydroxyl radical at the cavity collapse ($\propto \frac{m_{OH}}{V_{in}}$).

If concentration of pollutant is much smaller than C_S and $k_S \sim k_2$, we can simplify this equation as:

$$\emptyset = \alpha\,\epsilon_{GR}\left(\frac{C_{OH}}{C_S}\right) \qquad (10)$$

Where α is a proportionality constant. The concentration of scavangers may be assumed as constant and may be lumped with the proportionality constant. For the sake of dimensional consistency, C_S may be assumed to be 1 kmol/m^3.

The presented model provides a direct link between the key flow characteristics of the cavitation device/ reactor and the overall performance of cavitation reactor. The values of gas volume fractions appearing in Equation (10) may be obtained from CFD models of the cavitation device. C_{OH} may be estimated by solving cavity dynamics models. The overall approach of coupling CFD and cavity dynamics models with the per – pass degradation model is shown in Figure 2. Details of CFD and cavity dynamics models are briefly discussed in the following sub-sections.

3.1 CFD model of vortex based cavitation devices

The single phase flow characteristics of vortex diodes has been carried out previously by Pandare & Ranade (2015), they presented a detailed description of the key flow features and complexities. The vortex core formed through the central axis of the device exhibits unsteady behaviour, featuring a precession which was found to oscillate at a frequency of the order of 60 Hz. Along the axial port there is also a significant core of reverse flow, which persists for up to 30 diameters of the downstream pipework. As a result, the computational demands of full 3D CFD approaches are relatively high, requiring the resolution of small temporal and spatial scales (time steps of 10^{-6} s / near wall cell heights of ~50 μm). In the cavitation devices used in this work, mass transfer in the low pressure region generates a gas/ vapour core. This generation of multiphase flow with phase change increases the computational demands even further. In order to study multiphase flow in vortex based devices, it is therefore necessary to develop suitable, simplified 2D CFD models which open up the possibility to investigate a greater range of parameters in terms of operating conditions and device geometries.

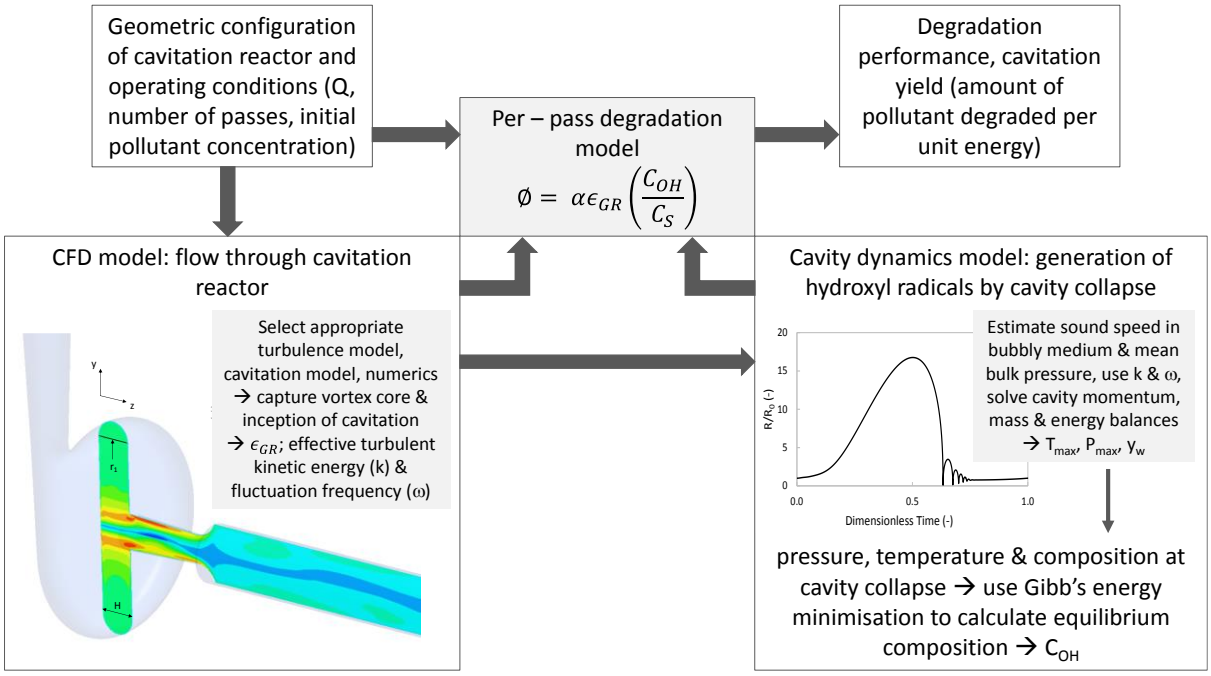

Figure 2: Approach for modelling of hydrodynamic cavitation reactors

In this work, we used the results presented by Simpson and Ranade (2018b). They have used detailed 3D simulations to formulate appropriate boundary conditions in terms of inlet tangential velocity and turbulence profiles for the 2D axis-symmetric models. Adopting an axis-symmetric approach omits some of the details and complexities observed in 3D, such as vortex precession. However, these omissions are acceptable in this first attempt of using CFD models for simulating the performance of vortex based hydrodynamic cavitation devices. Simpson and Ranade (2018b) were able to obtain good agreement with the pressure drop as well as the maximum tangential velocities predicted by full 3D simulations. It was also shown that the 2D simulations could successfully reproduce experimental pressure drops and cavitation inception points at different scales using the Singhal model (Singhal et al. 2002) and also capture key flow features. Full details of the 2D modelling approach, model equations, and numerical results are discussed by Simpson and Ranade (2018b) and are not included here for the sake of brevity. How the simulated results from CFD were used for estimating per-pass degradation performance of cavitation reactor are discussed in Section 4.

3.2 Cavity dynamics models to estimate generation of hydroxyl radicals

Cavities generated in the regions of pressure lower than vapour pressure of water oscillate as they travel through turbulent flow field, and eventually collapse generating very high localised pressure and temperature. The dynamics of these oscillating cavities is usually modelled using the classical Rayleigh-Plesset equation or its variants, which include various corrections (Hickling and Plesset, 1964; Keller and Miksis, 1980; Prosperetti and Lezzi, 1986). The Keller Miksis equation has been used in the present work to model cavity dynamics following Gireesan and Pandit (2017) and Pawar et al. (2017). The mass, momentum and energy balance equations used for simulating cavity dynamics are not discussed here for the sake of brevity and were taken from Gireesan and Pandit (2017).

The solution of the cavity dynamics models require the following input parameters:

- Initial cavity radius, R_0: Nucleation will generally lead to a distribution of initial cavity radii under the cavitating conditions. However, for the sake of simplicity and in absence of any

definitive information, in this work we have represented the cavity distribution by a single effective cavity radius. The cavity radius may therefore be treated as an adjustable parameter. This will be discussed in Section 4 in more details.

- Bulk pressure, P^B: The cavities will travel through the turbulent flow field and CFD models can provide the bulk pressure experienced by the cavities. This will be discussed in Section 4.
- Initial composition: The cavity at time zero will be assumed to contain air (desorbed from the water) following normal practice.

Another important parameter appearing in the cavity dynamics equations is the speed of sound, c. It is well known that sound speed in water is a strong function of bubble content. In order to account for this, the following equation proposed by Wilson and Roy (2008) was used to estimate the speed of sound in bubbly flow, denoted as c_{mlf}:

$$\frac{1}{c_{mlf}^2} = \frac{(1-\epsilon_{GR})^2}{c^2} + \frac{{\epsilon_{GR}}^2}{c_v^2} + \epsilon_{GR}(1-\epsilon_{GR})\frac{\rho_v^2 c_v^2 + \rho^2 c^2}{\rho \rho_v c^2 c_v^2} \qquad (11)$$

The reduction in speed of sound reduces the intensity of collapse and lowers the production of hydroxyl radicals. The solution of cavity dynamics equations provide the pressure, temperature and composition at the collapse. These results were used to simulate hydroxyl radical concentration by assuming equilibrium at collapse conditions (using Gibbs free energy minimisation similar to Krishnan et al. (2006) and Sivasankar and Moholkar (2008)). An online software – FactSage (a thermochemical software/database) was used for this purpose akin to the works of Pawar et al (2017).

4. Results and discussion

4.1 Degradation performance of vortex based cavitation reactor

Like many other cavitation devices, the vortex based cavitation reactor also exhibits a maxima in degradation rate with respect to the flow rate (or pressure drop across) the reactor. At very low flow rates (characterised by superficial velocity at the throat of the vortex based cavitation device as less

than 1 m/s), flow is not adequate to generate cavitation. As flow rate crosses an inception point, the cavitation occurs and we start getting non-zero per-pass degradation factors (see Sarvothaman et al. 2018 for more detailed discussion). Sarvothaman et al. (2018) have used a non-isothermal model to describe the experimental data. In order to simplify, in this work we considered only the nearly isothermal region of their data, and reprocessed the data to estimate an isothermal per-pass degradation factor. The results are shown in Figure 3. It can be seen that the degradation performance exhibits a maxima with respect to throat velocity. Increase in throat velocity beyond 3 m/s was found to reduce per-pass degradation performance. Similar observations regarding the existence of a maxima in degradation performance with respect to pressure drop has been reported by earlier works for conventional devices (Carpenter et al. 2017).

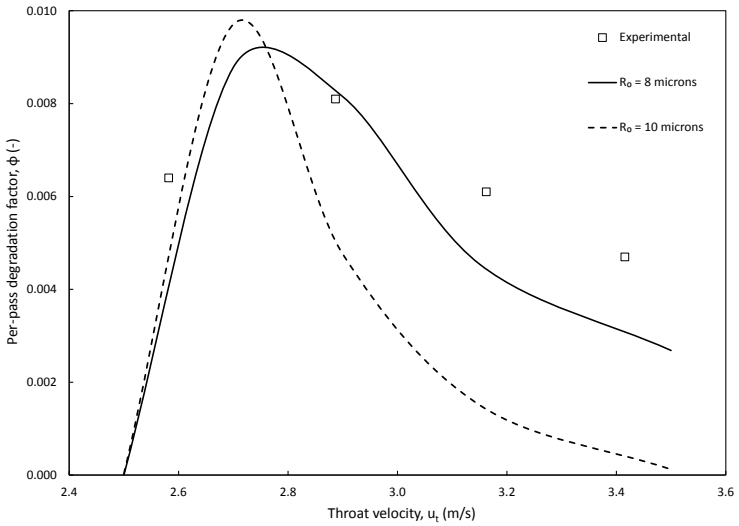

Figure 3: Influence of throat velocity on performance of cavitation reactor (experimental data from Sarvothaman et al. 2018 reprocessed using Equation 3 considering nearly isothermal region)

The task is now to see whether multi-layer models discussed earlier can help us to estimate this behaviour.

4.2 Estimation of ϕ

The first task in estimating ϕ is to use CFD models to quantify cavity trajectories and the pressure and turbulence experienced by cavities. This information is needed by the cavity dynamics models for

estimating the generation of hydroxyl radicals. The volume fraction of cavities, ϵ_{GR} is needed not only to estimate number of cavitation events but also to estimate effective sound speed in the region where cavities are collapsing. It is therefore essential to identify the relevant region in the cavitation reactor where cavities are generated and collapsed.

In the vortex based cavitation devices considered in this work, the inlet stream enters via tangential inlet. The conservation of momentum causes a significant increase in tangential velocity as the liquid moves towards the centre of the vortex chamber. This increase in tangential velocity leads to a low pressure region at the core of the vortex which is extended towards the axial port as the liquid exits the chamber. This low pressure region causes desorption of dissolved gases as well as under certain conditions, generation of cavitation (evaporation of water). The desorbed gas and generated vapours form a gaseous core at the centre of the vortex. This is clearly captured in the CFD models of Simpson and Ranade (2018b). A sample of results in the form of contours of gas volume fraction are shown in Figure 4a.

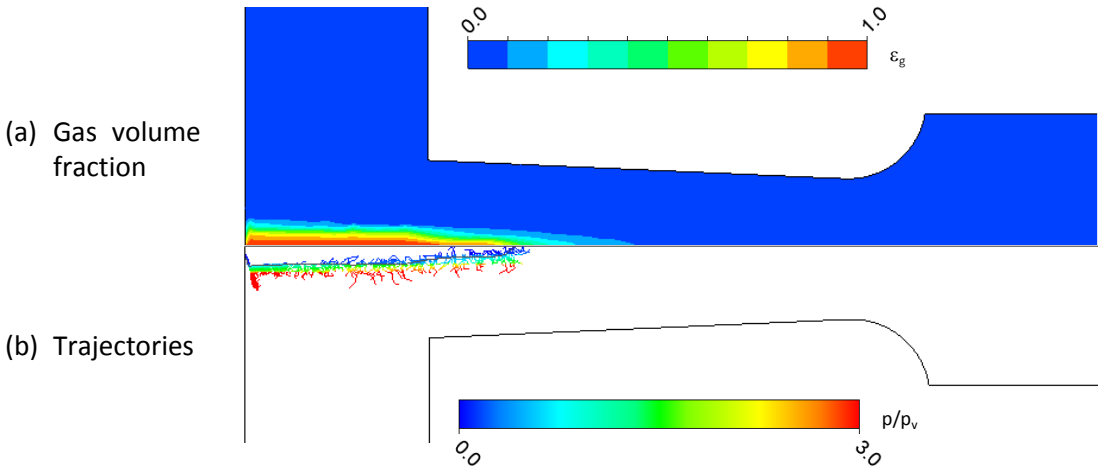

Figure 4: A sample of simulated results using the CFD model
6 mm cavitation device, throat velocity = 3 m/s, pressure drop = 250 kPa

It can be seen that formation of the gas core is captured correctly by the CFD models. The cavities are generated in this low pressure region – at the core of the vortex. These cavities then travel away from the core following the turbulent fluctuations of the flow. In order to understand the region over which cavities travel and collapse, it will be useful to examine relevant time and space scales.

The results from cavity dynamics models typically indicate cavity lifetimes of the order of $2x10^{-4}$ s, which translate to cavities travelling distances of the order of ~ 1 – 2 mm from inception to collapse. To illustrate these relatively short travel distances, sample results of simulated trajectories released from an iso-surface of constant vapour volume fraction (0.5) for the time of $2x10^{-4}$ s are shown in Figure 4b. The trajectories are coloured by the ratio of absolute pressure and vapour pressure, indicating that the maximum pressure recovery attained by the cavities prior to final collapse is typically less than three times of vapour pressure over these travel distances.

It should be noted that the source and sink terms used in the cavitation model considered in the CFD model are based on approximated cavity dynamics equations. Therefore, the simulated distribution of gas volume fractions using the CFD model can also be used to quantify the relevant region of generation of cavities and collapsing cavities. Considering that the CFD models used in this work are based on the Eulerian framework and do not explicitly account for coalescence of cavities to form a gas core, some approximation is needed to identify the gas core. Earlier studies on multiphase flows with the Eulerian models have used a cut off of gas volume fractions ranging from 0.5 to 0.66 for identifying gas-liquid interface (Ranade, 2002). Following those, in this work we have set a volume fraction of 0.5 to identify a boundary of gas core and dispersion. We assume that cavities are generated on the surface of this identified gas core.

The generated cavities travel in the regions of high pressure through the turbulent flow field and eventually collapse. As cavities collapse, the volume fraction of gas starts reducing. Beyond a certain

collapsing zone, the gas volume fraction will be virtually zero. In this work we have assumed the outer boundary of the cavity collapse region to correspond to a cut off of gas volume fraction of 0.1. Of course, there will be some cavities which may travel beyond this region. However, most of the cavities may be assumed to be collapsed in this region. The boundaries of the gas core and cavity collapse region based on this assumed cut off in gas volume fraction are shown in Figure 5.

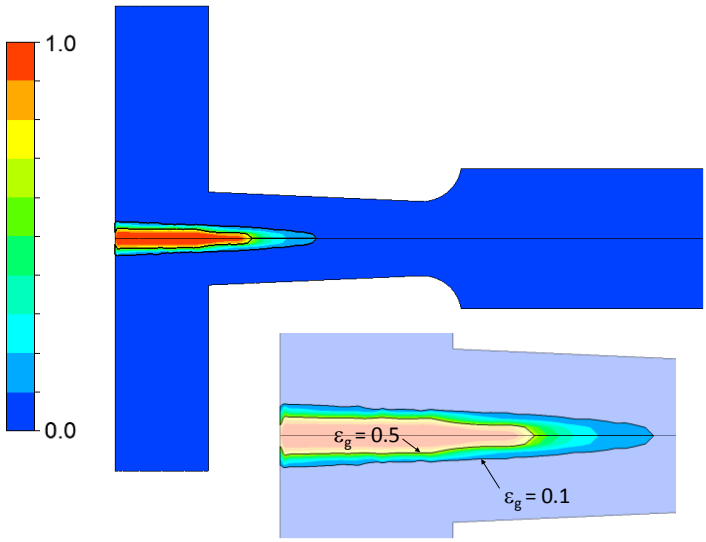

Figure 5: Regions of gas core (ϵ_G > 0.5) and cavity collapse (0.5 > ϵ_G > 0.1)
6 mm cavitation device, throat velocity = 3 m/s, pressure drop = 250 kPa

Once we identify the region of collapsing cavities, one may use the simulated CFD results to estimate the relevant quantities of interest. The volume fraction of cavities, ϵ_{GR} required for estimating number of cavitation units as well as effective sound speed in the collapsing region can then be calculated from the CFD simulations for a range of operating flow rates, and for different device scales. The average volume fraction of gas in the cavity collapsing region (0.5 > ϵ_G > 0.1), is shown in Figure 6.

It can be seen that gas volume fraction in the region of interest is independent of device scale, and increases with liquid flow rate (throat velocity). Beyond a certain increase in throat velocity, gas volume fraction appears to plateau. This predicted gas hold up was then used with Equation (10) to determine the per – pass degradation factor.

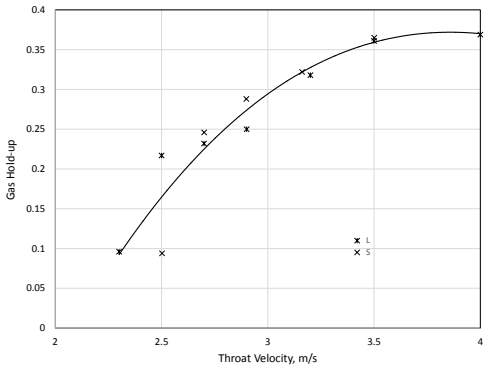

Figure 6: Simulated average gas volume fraction ϵ_{GR} in the cavity collapsing region

The next important task is to estimate the bulk pressure and its fluctuations experienced by the cavities. It is in principle possible to use the Lagrangian framework using the simulated flow field to track the trajectories of the cavities. These Lagrangian trajectory simulations involve approximations of turbulent time scales (Ranade, 2002). Considering the relatively small region of cavity collapse, instead of tracking the cavities in the Lagrangian framework, we approximated the fluctuations in the bulk pressure experienced by the cavity as:

$$P^B = f\, P_v + \rho\, k_R\, sin(\omega_R\, t) \qquad (12)$$

Where 'f' is an empirical parameter, k_R and ω_R are average turbulent kinetic energy and turbulent frequency in the cavity collapse region, R. It can be seen that the amplitude of pressure fluctuations is proportional to the turbulent kinetic energy, and the frequency of pressure fluctuations is directly related to turbulent eddy frequency. Typical distribution of turbulent kinetic energy and turbulent frequency in the cavitation device are shown in Figure 7.

The volume averaged values of turbulent kinetic energy and turbulent frequency over the identified cavity collapse region, R, were critically analysed to understand the observed trends. As a sample of results, the simulated values of average turbulent kinetic energy are shown in Figure 8 for the two sizes of cavitation devices (small, S and large, L). It can be seen that simulated values of turbulent

kinetic energy are not a function of device scales. As expected, turbulent kinetic energy increases with increase in throat velocity. The value of turbulent kinetic energy and turbulent frequency were found to exhibit following trends:

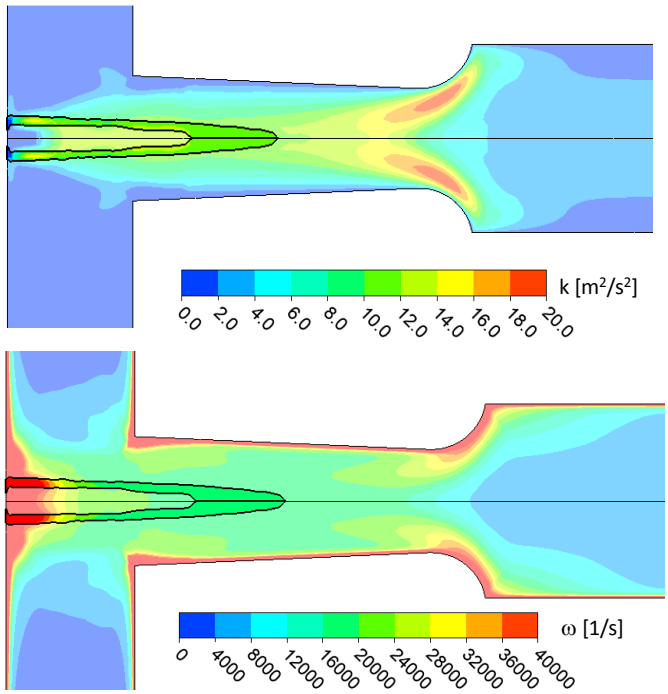

Figure 7: Simulated contours of turbulent kinetic energy and turbulent frequency in the region of interest [6 mm cavitation device, throat velocity = 3 m/s]

$$k = a + b\,(u_t - u_{tc})^2 \qquad (13)$$

and

$$\omega = \frac{c}{d_t}\,(u_t - d) \qquad (14)$$

Where values of a, b, c, d and u_{tc} are independent of device scale. The values of a, b and u_{tc} are approximately 10 m^2/s^2, 4.5, 1.4 m/s and 2.5 m/s.

As the cavity collapse time scales are small, the mean bulk pressure variation is also quite small. The value of f appearing in the Equation (15) is estimated to be close to 1. In order to understand the

sensitivity towards mean bulk pressure, for a specific set of R_0, k_R and ω_R, the influence of mean bulk pressure (value of f) on simulated values of per – pass degradation factor was investigated. These results are shown in Figure 9. It can be seen that the values of per – pass degradation factor are not unduly sensitive to the value of f.

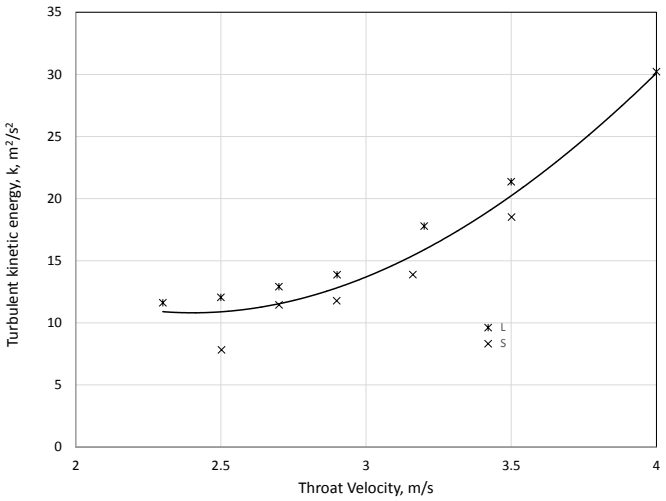

Figure 8: Simulated average turbulent kinetic energy, k_R in the cavity collapsing region

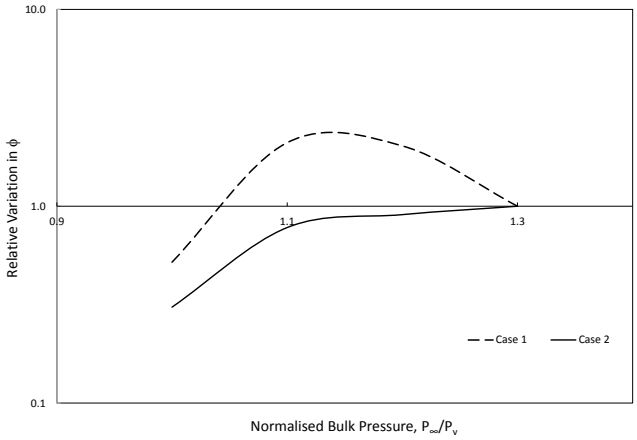

Figure 9: Sensitivity towards normalised bulk pressure
(R_0= XX micron, Case 1: k_R = 4.8 m^2/s^2 and ω_R= 6.6 kHz; Case 2: k_R = 8 m^2/s^2 and ω_R= 4.2 kHz)

Considering the relative insensitivity towards the mean bulk pressure, all the subsequent cavity dynamics simulations were carried out by setting the mean bulk pressure equal to the vapour pressure.

With this, all the necessary quantities for simulating cavity dynamics model to estimate C_{OH} and therefore to estimate per – pass degradation factor are available from the CFD model. Using these values, the simulated per – pass degradation factors are shown in Figure 3. The proportionality factor was found to be 8 x 10^7 which was kept constant for all the subsequent calculations. It can be seen that the estimated values of per – pass degradation factor are a function of initial cavity size. The estimated results shown by continuous curves in Figure 3 were calculated by assuming the same initial cavity size for all the operating conditions. It may be possible to obtain a better fit with the experimental data if different values of initial cavity size are used for different throat velocities. The sensitivity of the estimated per – pass degradation factor with the initial cavity size for the case of throat velocity of 3.5 m/s is shown in Figure 10. It can be seen that instead of 8 micron, if cavity size is assumed to be 7.5 micron for 3.5 m/s case, estimated value agrees with the experimental data. Higher throat velocity requires reduced initial cavity size.

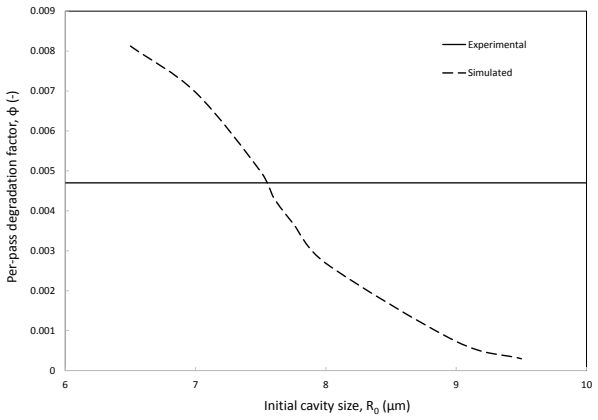

Figure 10: Influence of initial cavity size on estimated per – pass degradation factor
6 mm throat diameter, 3.5 m/s throat velocity, pressure drop = 350 kPa

However, considering the uncertainties involved in estimating variation of initial cavity size with operating conditions, in this work we decided not to consider variation of R_0 as a function of throat velocity. The simulated values of per – pass degradation factor shown in Figure 4 with 8 micron initial cavity size may be considered reasonable owing to the fact that there is only one adjustable parameter involved in these estimations.

The combination of CFD, cavity dynamics and per – pass degradation model appears to describe the experimental data reasonably well with the help of one adjustable parameter. Considering the complexities involving a wide range of length and time scales, the approach can be considered successful. It is important to evaluate possible extensions of this approach to explore performance enhancements of cavitation reactor and possibly scale – up. Such an attempt is made here.

4.3 Application of the developed model for optimisation and scale – up

In order to enhance application horizons of hydrodynamic cavitation reactors and processes, it is important to develop a systematic modelling framework for design and interpretation of the data like the one described in previous section. It is even more important to use these models to gain insights into the underlying processes in hydrodynamic cavitation reactors so that new ideas for improving performance can be evolved. The models can also be used to gain a better understanding of scale – up issues associated with hydrodynamic cavitation reactors. The results discussed so far demonstrate the possibility of increasing per – pass degradation performance of the hydrodynamic cavitation reactor by appropriately choosing operating conditions. In all cases considered so far, the downstream pressure of the cavitation reactor was atmospheric. Recently, Soyama and Hoshino (2016) have reported that for a constant upstream pressure, increase in the downstream pressure improved the cavitation performance of a venturi. They also reported that increase in downstream pressure reduces extent of cavitation. In this work, we decided to investigate this.

As discussed in Section 2, the downstream pressure for a given upstream pressure was manipulated by adjusting valves downstream of the cavitation reactor. Here we considered only a case of upstream pressure of 300 kPa (gauge) as an example. For this upstream pressure, downstream pressure was increased to 100 kPag (effectively pressure drop across the cavitation reactor was 200 kPa). The observed degradation performance is shown in Figure 11. It can be seen that the increase in downstream pressure to 100 kPag substantially improved the degradation performance.

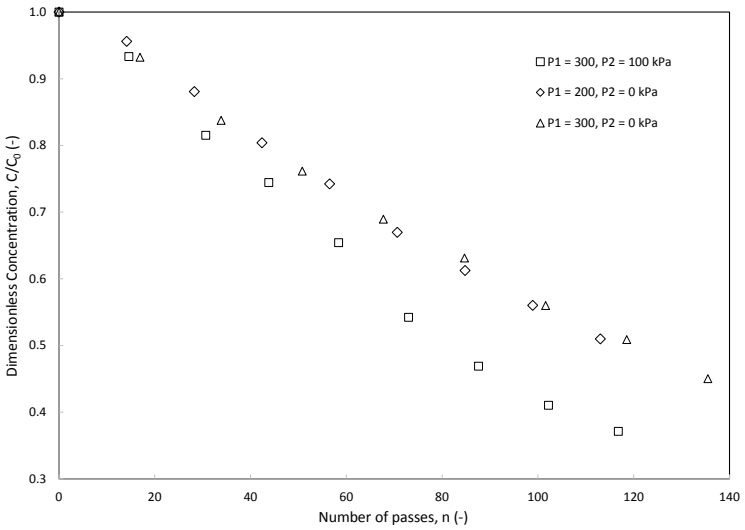

Figure 11: Influence of downstream pressure on degradation
6 mm throat reactor, acetone contaminated water, initial concentration: ~ 1000 ppm

The degradation performance of cavitation reactor with an effective pressure drop across reactor of 200 kPa but with atmospheric downstream pressure is also shown in Figure 11. It can be seen that the operation with enhanced downstream pressure performs better than the other two cases with atmospheric downstream pressure.

Attempt was made to interpret these results using the model developed in this work. Since the pressure drop across the cavitation reactor for 300 kPag upstream – 100 kPag downstream case and for 200 kPag upstream – 0 kPag downstream case is the same, the flow field will also be the same. One may therefore use the averaged turbulent kinetic energy, k_R and turbulent frequency, ω_R from the earlier CFD results for simulating the new case with higher downstream pressure. The higher downstream pressure however will reduce the extent of cavitation. It is therefore essential to carry out a separate CFD simulation to correctly reflect the operating conditions. This was carried out and the CFD model correctly captured by the reduction in the extent of cavitation. The value of gas volume fraction in the region of interest reduced from 0.24 to ~ 0.05 (shown in Figure 12 b). No quantitative experimental data is available to evaluate these simulations. However, the simulations at least

captured the trend correctly. As expected the averaged turbulent kinetic energy, k_R and turbulent frequency, ω_R were found to quite similar to the case with corresponding pressure drop with atmospheric downstream pressure. Using the values from the CFD model, the multi-layer model discussed earlier was used to estimate influence of downstream pressure. The simulated results are shown in Figure 12 a.

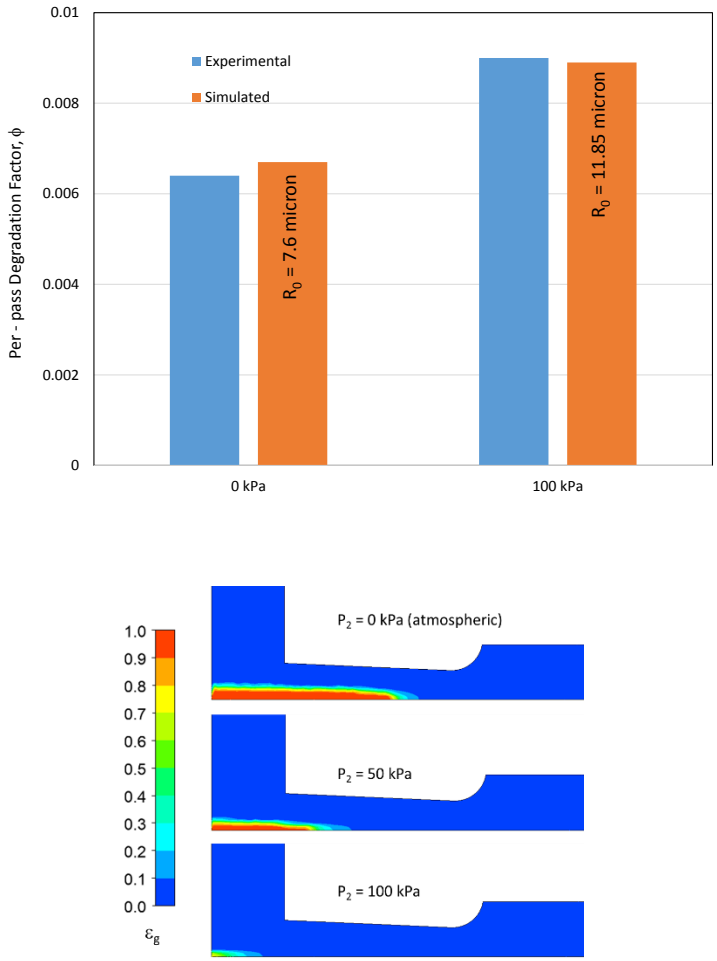

Figure 12: (a) Influence of downstream pressure on per – pass degradation factor
6 mm throat reactor, upstream pressure= 300 kPa, (b) CFD contours for 6 mm throat reactor, upstream pressure = 300 kPa

It can be seen that in order to match the observed performance enhancement, the effective initial cavity size had to be increased from ~ 8 micron to ~ 12 micron. Increase in downstream pressure will reduce the effective driving force for cavitation – which may enhance initial effective cavity size. The results therefore look qualitatively reasonable. The results indicate that overall degradation

performance of cavitation reactor may be enhanced by manipulating downstream pressure. More insights into how effective cavity size can be influenced will allow new ideas for possible performance enhancement.

Another important application of the model is in understanding scale – up of the cavitation reactor. Not much information on scale – up of cavitation reactor is available. Sarvothaman et al. (2018) have reported one of the first data on geometrically similar cavitation reactors of two different sizes. Despite some of the uncertainties in estimating effective initial cavity size, we attempted to apply the model for understanding scale – up of cavitation reactors. As an example, we discuss here the case of one specific throat velocity (~ 3 m/s). Maintaining the same throat velocity realises almost the same pressure drop across the reactor. This has been confirmed from the experimental data as well as from the CFD simulations. The gas volume fraction and turbulent kinetic energy were also not found to be functions of device scale (see Section 4.2). The turbulent frequency was found to be inversely proportional to device scale (throat diameter). Cavity dynamics model results had indicated that a reduction in turbulent frequency allows more time for the cavities to grow, and therefore leads to enhanced generation of radical production. However, the experimental data reported by Sarvothaman et al. (2018) indicated that performance of a larger reactor (12 mm throat diameter) with scale – up factor of 4 was inferior to the smaller reactor (6 mm throat diameter). The computational models developed here were used to understand these results. CFD simulations were carried out for the larger scale cavitation reactor. Though experimental data was not available for the cavitation reactor with throat diameter of 24 mm, CFD simulations were carried out for the purpose of gaining insights into the potential effects of scale – up. Idea was to use the model to gain understanding and insight about potential effect of scale – up. Following the approach discussed in Section 4.2, the effective initial cavity size was treated as an adjustable parameter. The simulated results and their comparison with the experimental data is shown in Figure 13.

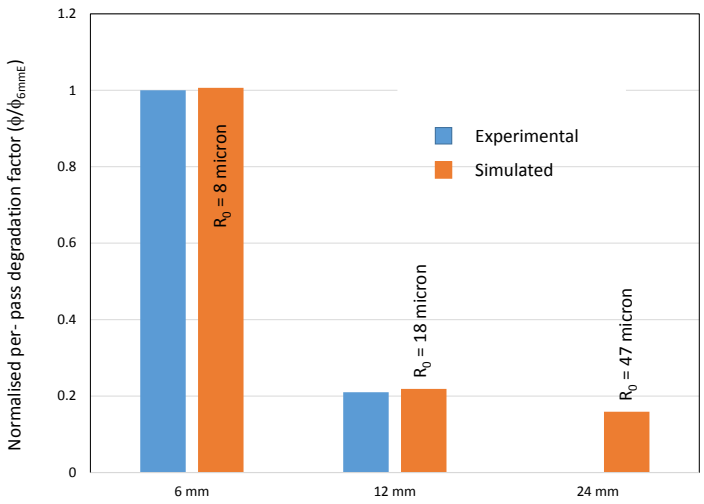

Figure 13: Influence of scale on per – pass degradation factor

It can be seen that effective cavity size had to be increased to match the experimental data for the larger cavitation reactor (8 micron for the smaller reactor to 18 micron for the larger reactor). The experimental data on the performance of even larger cavitation reactor is not yet available in open literature. The limited experimental data used in this work indicates significant difference in the degradation performance with cavitation reactor of characteristic dimension of 12 mm (nominal capacity of 1.2 m^3/hr) and 6 mm (nominal capacity of 0.3 m^3/hr). However, similar cavitation devices have been scaled – up following a simple dynamic similarity scaling up to 50 m^3/hr which indicates that further increase in scale – up does not exhibit drastic reduction in performance with scale (Utikar, 2018). The smaller cavitation reactor (with characteristic dimension of 6 mm) appears to operate in a different regime than the larger cavitation reactors. However, further work, particularly, detailed experimental characterisation of cavitation in smaller and larger cavitation reactors is essential for drawing firmer conclusions. The simulations using the presented model indicate that if effective initial cavity size is assumed to exhibit similar increase with scale, the performance of the 24 mm throat diameter will not be significantly inferior to that of 12 mm throat diameter. Effective initial size of cavity as 47 micron for the reactor with 24 mm throat diameter resulted in more or less same per – pass degradation factor as that of reactor with 12 mm throat diameter.

The influence of turbulent frequency (which reduced with increase in reactor scale for a specific throat velocity) and effective initial cavity size is quite complex and cannot be estimated by simple relationships. It is essential to couple the CFD model and cavity dynamics model to get a better understanding of possible influence of variety of design and operating parameters. Further work on detailed transient 3D simulations of cavitating flows in vortex based devices is in progress. We hope that this on-going work will help us to unravel key insights on why there is a significant difference in the cavitation reactors with characteristics dimensions of 6 mm and 12 mm but not significant difference in devices with 12 mm and larger dimensions.

The wider application of the presented modelling framework appears to be limited at the moment by the lack of a better understanding of the estimation of effective initial cavity size. However, despite this limitation, the developed framework for the first time established direct connection between per – pass degradation performance of a cavitation reactor with underlying device scale flow characteristics and cavity dynamics. Further investigation into nucleation and the physics of phase transfer during cavitation will lead to a better understanding and improve our ability to estimate effective initial cavity size. It is also possible to extend the developed framework to consider cavity size distribution in a straightforward manner. We therefore believe that the modelling framework presented here is quite promising and will eventually lead to a comprehensive framework for the design, optimisation and scale – up of hydrodynamic cavitation reactors.

5. Summary & Conclusions

A systematic framework has been developed to estimate the per-pass degradation performance of a vortex based cavitation reactor. The presented modelling approach integrates micro-scale cavity dynamics calculations and reactor scale, multiphase CFD calculations into an overall process model to predict the value of ϕ, the per-pass degradation factor. In absence of definitive data or information

about the initial cavity sizes & size distribution formed by cavitation, the resulting model involves the use of the initial bubble radius, R_0, as a single adjustable parameter. The model was found to successfully reproduce experimental trends, replicating the maxima with respect to throat velocity (or pressure drop across cavitation reactor) observed in measured degradation performance. Subsequently the model was applied to predict performance at different device scales, and also at different back pressures (downstream pressures). It was found that adjustment of the initial radius was required in order to reproduce performance trends at different device scales, as well as performance with increased applied back pressure. Specific highlights of this study may be summarised as:

- CFD models were able to capture formation of gaseous central core and identify the relevant region for collapsing cavities in the vortex based cavitation reactor. The average gas volume fraction and turbulent kinetic energy in this identified region were not found to be dependent on the scale of the reactor. The average turbulent frequency in this identified region was found to be inversely proportional to the reactor scale.
- The estimated values of per – pass degradation factor were quite sensitive to the turbulent frequency and effective initial cavity size.
- The approach presented in this work based on CFD models and cavity dynamics models was able to simulate per – pass degradation performance with the help of a one adjustable parameter (initial cavity size, R_0).
- Increased downstream pressure for the constant upstream pressure of 300 kPag was found to improve the performance. Larger effective initial cavity size is required to fit the influence of increased downstream pressure.
- Per – pass degradation performance was found to decrease with scale of cavitation reactor based on the two scales investigated here. Larger effective initial cavity size is required to fit the influence of increased reactor scale. Further work is needed to understand influence of scale on performance of cavitation reactor.

Predictions have been shown to be sensitive to the choice of initial bubble radius, suggesting that controlling the size and size distribution is itself an important consideration in performance optimisation. The presented multi-layer modelling framework provides a sound basis for further development of multi-scale predictive models to design, optimise and scale – up of hydrodynamic cavitation reactors.

Acknowledgements:

Authors gratefully acknowledge the funding support from the start-up grant G1013CHM of Queen's University Belfast, UK.

Notation

c_l	Speed of sound in liquid medium (m/s)
c_v	Speed of sound in gas medium (m/s)
c_{mlf}	Speed of sound in multiphase flow (m/s)
C	Outlet concentration for industrial cavitation setup (µmol/m^3)
C_{in}	Inlet concentration for industrial cavitation setup (µmol/m^3)
C_{OH}	Concentration of hydroxyl radical at collapse (kmol/m^3)
C_S	Concentration of scavengers (kmol/m^3)
C_1	constant coefficient 1
C_2	constant coefficient 2
f_v	Vapour mass fraction (-)
f_g	Non-condensable gas mass fraction (-)
G	Generation rate of hydroxyl radicals (kmol/s)
k	turbulence kinetic energy (m^2/s^2)
k_2	Second order rate constant (M^{-1} s^{-1})

k_s	Second order rate constant of reaction between hydroxyl radicals and other reactants than pollutant of interest (M^{-1} s^{-1})
L	Large cavitation device
m_{OH}	Hydroxyl radicals generated per collapse (kmol/s)
n_p	Number of passes through cavitation device (-)
n	Number of collapsing cavities per second (s^{-1})
Q	Recirculating flow through cavitation device (m^3/s)
R_e	evaporation mass transfer rate source term
R_c	condensation mass transfer rate source term
S	Small cavitation device
T	Bulk temperature, (K)
V	Volume of holding tank (m^3)
V_{in}	Volume of cavity at inception (m^3)
v_t	Throat velocity (m/s)
p	pressure (absolute) (Pa)
p_v	saturated vapour pressure (Pa)
ΔP	Pressure drop across cavitation device (kPa)
α	Proportionality constant (-)
β	Ratio of flow rate through cavitation device (Q) and holding tank volume (V) (s^{-1})
δ	Fraction of generated radicals utilised for pollutant degradation (-)
ϵ_{GR}	Gas volume fraction (-)
ϕ	Per-pass degradation factor (-)
ρ	Liquid density (kg/m^3)
ρ_v	Vapour density (kg/m^3)
σ	Surface tension (Ns/m^2)
τ	Residence time of liquid in holding tank (s)

References

Arrojo, S. and Benito, Y., 2008. A theoretical study of hydrodynamic cavitation. *Ultrasonics Sonochemistry*, **15(3)**: 203-211.

Barik, A.J. and Gogate, P.R., 2016. Degradation of 4-chloro 2-aminophenol using a novel combined process based on hydrodynamic cavitation, UV photolysis and ozone. Ultrasonics sonochemistry, **30**: 70-78.

Carpenter, J., Badve, M., Rajoriya, S., George, S., Saharan, V.K. and Pandit, A.B., 2017. Hydrodynamic cavitation: an emerging technology for the intensification of various chemical and physical processes in a chemical process industry. *Reviews in Chemical Engineering*, **33(5)**: 433-468.

Capocelli, M., Prisciandaro, M., Lancia, A. and Musmarra, D., 2014. Hydrodynamic cavitation of p-nitrophenol: a theoretical and experimental insight. *Chemical Engineering Journal*, **254**: 1-8.

Chakinala, A.G., Gogate, P.R., Burgess, A.E. and Bremner, D.H., 2009. Industrial wastewater treatment using hydrodynamic cavitation and heterogeneous advanced Fenton processing. *Chemical Engineering Journal*, **152(2-3)**: 498-502.

Chakma, S. and Moholkar, V.S., 2013. Numerical simulation and investigation of system parameters of sonochemical process. *Chinese Journal of Engineering*, (1-14): ID362682.

Gągol, M., Przyjazny, A. and Boczkaj, G., 2018. Wastewater treatment by means of advanced oxidation processes based on cavitation–A Review. *Chemical Engineering Journal*, **338**: 599-627.

Gireesan, S. and Pandit, A.B., 2017. Modeling the effect of carbon-dioxide gas on cavitation. *Ultrasonics sonochemistry*, **34:** 721-728.

Gogate, P.R. and Pandit, A.B., 2001. Hydrodynamic cavitation reactors: a state of the art review. *Reviews in chemical engineering*, **17(1)**: 1-85.

Hsiao, C.T., Ma, J. and Chahine, G.L., 2017. Multiscale tow-phase flow modeling of sheet and cloud cavitation. *International Journal of Multiphase Flow*, **90**: 102-117.

Ma, J., Hsiao, C.T. and Chahine, G.L., 2017. A physics based multiscale modeling of cavitating flows. *Computers & Fluids*, **145**: 68-84.

Jyoti, K.K. and Pandit, A.B., 2001. Water disinfection by acoustic and hydrodynamic cavitation. *Biochemical Engineering Journal*, **7(3)**: 201-212.

Kanthale, P.M., Gogate, P.R., Pandit, A.B. and Wilhelm, A.M., 2005. Dynamics of cavitational bubbles and design of a hydrodynamic cavitational reactor: cluster approach. *Ultrasonics sonochemistry*, **12(6)**: 441-452.

Krishnan, J. S., Prashant Dwivedi and Vijayanand S. Moholkar. 2006. Numerical Investigation into the Chemistry Induced by Hydrodynamic Cavitation. *Industrial & Engineering Chemistry Research*, **45**:1493-1504.

Liu Z, Brenner CE. Models of cavitation event rate. In: Proceedings of CAV95 International Symposium of Cavitation, Deauville, France, 1995:321–328.

Moholkar, V.S. and Pandit, A.B., 1997. Bubble behavior in hydrodynamic cavitation: effect of turbulence. *AIChE Journal*, **43(6)**: 1641-1648.

Moholkar, V.S. and Pandit, A.B., 2001a. Modeling of hydrodynamic cavitation reactors: a unified approach. *Chemical engineering science*, **56(21-22)**: 6295-6302.

Moholkar, V.S. and Pandit, A.B., 2001b. Numerical investigations in the behaviour of one-dimensional bubbly flow in hydrodynamic cavitation. *Chemical Engineering Science*, **56(4)**: 1411-1418.

Naidu, DV P., R. Rajan, R. Kumar, KS Gandhi, VH Arakeri and S. Chandrasekaran. 1994. Modelling of a Batch Sonochemical Reactor. *Chemical Engineering Science*, **49 (6)**: 877- 888.

Pathania, S., Ho, Q.T., Hogan, S.A., McCarthy, N. and Tobin, J.T., 2018. Applications of hydrodynamic cavitation for instant rehydration of high protein milk powders. *Journal of Food Engineering*, **225**: 18-25.

Pawar, Sandip K., Amit V. Mahulkar, Kuldeep Roy, Vijananand S. Moholkar and Aniruddha B. Pandit. 2017. Sonochemical Effect Induced by Hydrodynamic Cavitation: Comparison of Venturi/Orifice Flow Geometries. *AIChE Journal*, **63**: 4705 – 4716.

Pandare, A. and Ranade, V.V., 2015. Flow in vortex diodes. *Chemical Engineering Research and Design*, **102**: 274-285.

Rajoriya, S., Bargole, S. and Saharan, V.K., 2017. Degradation of reactive blue 13 using hydrodynamic cavitation: Effect of geometrical parameters and different oxidizing additives. *Ultrasonics sonochemistry*, **37**: 192-202.

Rajoriya, S., Bargole, S., George, S. and Saharan, V.K., 2018. Treatment of textile dyeing industry effluent using hydrodynamic cavitation in combination with advanced oxidation reagents. *Journal of Hazardous Materials*, **344**: 1109-1115.

Ranade, V.V. and Bhandari, V.M., 2014. *Industrial wastewater treatment, recycling and reuse*. Butterworth-Heinemann.

Ranade, V.V., Kulkarni, A.A. and Bhandari, V.M., Council of Scientific and Industrial Research (CSIR), 2016. *Vortex diodes as effluent treatment devices*. U.S. Patent **9,422,952**.

Ranade, V.V., Kulkarni, A.A. and Bhandari, V.M., Council of Scientific and Industrial Research (CSIR), 2017. *Apparatus and method for reduction in ammoniacal nitrogen from waste waters*. U.S. Patent **9,725,338**.

Šarc, Andrej, Tadej Stepišnik-Perdih, Martin Petkovšek and Matevž Dular. 2017. The Issue of Cavitation Number Value in Studies of Water Treatment by Hydrodynamic Cavitation. *Ultrasonics sonochemistry,* **34**: 51-59.

Sarvothaman, V.P., Nagarajan, S. and Ranade, V.V., 2018. Treatment of Solvent Contaminated Water using Vortex based Cavitation: Influence of operating pressure drop, temperature, aeration and reactor scale. *Ind. Eng. Chem. Res.* **57** (28): 9292-9304.

Simpson, A. and V.V. Ranade. 2018a. Modelling of Hydrodynamic Cavitation with Orifice: Influence of different orifice designs, *Chemical Engineering Research & Design*, **136**: 698-711.

Simpson, A. and V.V. Ranade. 2018b. Cavitating Flows in a Vortex Unit: Computational Investigation on Influence of Operating Parameters and Scale, *AIChE Journal*, submitted.

Singhal, A.K., Athavale, M.M., Li, H. and Jiang, Y., 2002. Mathematical basis and validation of the full cavitation model. *Journal of fluids engineering*, ***124*(3)**: 617-624.

Sharma, Amit, Parag R. Gogate, Amit Mahulkar and Aniruddha B. Pandit. 2008. Modeling of Hydrodynamic Cavitation Reactors Based on Orifice Plates Considering Hydrodynamics and Chemical Reactions Occurring in Bubble. *Chemical Engineering Journal*, **143**: 201-209.

Sochard, S., Wilhelm, A.M. and Delmas, H., 1997. Modelling of free radicals production in a collapsing gas-vapour bubble. *Ultrasonics Sonochemistry*, **4(2)**: 77-84.

Sochard, S., Wilhelm, A.M. and Delmas, H., 1998. Gas-vapour bubble dynamics and homogeneous sonochemistry. *Chemical engineering science*, **53(2)**: 239-254.

Soyama, H. and Hoshino, J., 2016. Enhancing the aggressive intensity of hydrodynamic cavitation through a Venturi tube by increasing the pressure in the region where the bubbles collapse. *AIP Advances*, **6(4)**: 045113.

Suryawanshi, N.B., Bhandari, V.M., Sorokhaibam, L.G. and Ranade, V.V., 2017. Developing techno-economically sustainable methodologies for deep desulfurization using hydrodynamic cavitation. *Fuel*, **210**: 482-490.

Suryawanshi, Pravin G., Vinay M. Bhandari, Laxmi G. Sorokhaibam, Jayesh P. Ruparelia and Vivek V. Ranade. 2018. Solvent Degradation Studies using Hydrodynamic Cavitation. *Environmental Progress & Sustainable Energy,* **37**: 295-304.

Thanekar, P., Panda, M. and Gogate, P.R., 2018. Degradation of carbamazepine using hydrodynamic cavitation combined with advanced oxidation processes. *Ultrasonics sonochemistry*, **40**: 567-576.

Toegel, Ruediger, Sascha Hilgenfeldt and Detlef Lohse. 2002. Suppressing Dissociation in Sonoluminescing Bubbles: The Effect of Excluded Volume. *Physical Review Letters*, **88**: 034301.

Utikar, R.P. (2018), Private communications.

Wilson, P.S. and Roy, R.A., 2008. An audible demonstration of the speed of sound in bubbly liquids. *American Journal of Physics*, **76(10)**: 975-981.